RSC Advances

ROYAL SOCIETY OF CHEMISTRY

www.rsc.org/advances

Graphical Abstract

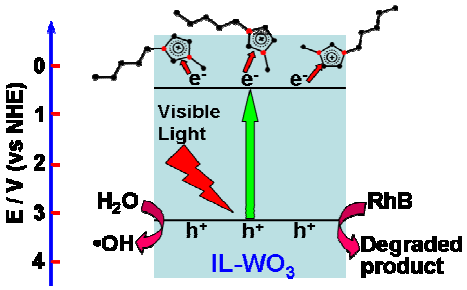

The ionic liquid (IL) modification endows the surface of WO_3 a stronger electron-trapping capability, which effectively inhibits the recombination of electron-hole pairs and thus enhances the photocatalysis.

Modification of Tungsten Trioxide with Ionic Liquid for Enhanced Photocatalytic Performance

Jingjing Liu, Suiqi Han, Jia Li and Jun Lin*

Department of Chemistry, Renmin University of China, Beijing 100872, People's Republic of China

Corresponding Author

*E-mail: jlin@chem.ruc.edu.cn; Tel: +86-10-62514133; Fax: +86-10-62516444.

Abstract

To develop WO_3, a narrow band gap semiconductor with a deep valence band, to be an efficient visible light photocatalyst, in this study, we modified WO_3 with an ionic liquid [Bmim]I through a facile impregnation method. Upon visible light irradiation, the [Bmim]I-modified WO_3 has been shown to have much higher photocatalytic activities than the unmodified counterpart for the degradation of RhB in aqueous solution. The effects of the ionic liquid modification on the physicochemical properties of WO_3 and the enhanced photocatalysis were investigated in detail according to the various characterizations and analysis of photogenerated hydroxyl radicals. It was revealed that the ionic liquid is bound to the surface of WO_3 after the modification. The presence of the surface-bound imidazolium ring was demonstrated to suppress the recombination of photoexcited electron-hole pairs effectively, resulting in the enhanced photocatalysis over the [Bmim]I-modified WO_3. Furthermore, the [Bmim]I-modified WO_3 exhibited sufficient stability and recyclability with respect to photocatalytic activity, which would made it a promising photocatalyst for a practical application.

Keywords: Visible Light Photocatalysis; Ionic Liquid Modification; WO_3; [Bmim]I; Narrow Band Gap semiconductor.

1. Introduction

For the full utilization of solar light, it has become a hot topic in photocatalysis scopes to develop narrow band gap semiconductors as efficient visible light photocatalytic materials in recent years.[1-3] Among various narrow band gap semiconductors, tungsten trioxide (WO_3) with a band gap of 2.6~2.8 eV has been attracting considerable attention due to its stable physicochemical properties, non-toxicity, resistance to photo corrosion, and especially its strong oxidation power of the holes photogenerated in the valence band (+3.1~3.2 V vs NHE).[4-8] However, owing to the low conduction band edge of WO_3 (+0.3~0.5 V vs NHE), the electrons photoexcited in the conduction band cannot be efficiently consumed by oxygen molecule through one-electron reduction process ($E^o(O_2/O_2^{-\bullet})$ =−0.33 V vs NHE), which results in the fast charge recombination and a poor photocatalytic performance. This low charge separation in WO_3 is a serious drawback in the development of WO_3 as an efficient visible light photocatalyst. Recently, great efforts have been undertaken to improve the photocatalytic performance of WO_3 for the degradation of organic pollutants and O_2 evolution. Typically, Pt-loaded WO_3 was reported to exhibit a high photocatalytic activity under visible light irradiation because the surface Pt promotes the multi-electron reduction of the adsorbed oxygen ($E^o(O_2/H_2O_2)$ = +0.695 V vs NHE and $E^o(O_2/2H_2O)$ = + 1.229 V vs NHE), giving a rise to the charge separation.[9,10] Subsequently, many studies on the morphology control of Pt/WO_3 and the surface modification of WO_3 with Pd, Pt/Au, CuO, Cu(II) clusters or graphene have been carried out.[11-16] Meanwhile, nanostructured WO_3 with controlled morphologies or microstructures was also demonstrated to have an enhanced photocatalytic activity due to large surface area and novel structure.[7,17] These works have made great contributions to the improvement of the photocatalytic performance of the narrow band gap semiconductor WO_3.

Ionic liquids (IL), as a new class of reaction media and solvents, have been extensively employed in organic synthesis, catalysis, separation, and CO_2 capture due to their unique characteristics such as thermal stability, negligible vapor pressure, high ionic conductivity, good dissolving ability, environmentally friendly feature, and wide electrochemical window.[18,19] The development of ionic liquids as green reaction media has also provided a lot of new opportunities for the synthesis and performance optimization of inorganic materials.[20] Recently, it was reported that the visible light photocatalytic activities of some semiconductors such as TiO_2 and BiOI can

be improved by the surface modification of ionic liquids.[21,22] To develop WO_3, a narrow band gap semiconductor with a deep valence band, as an efficient visible light photocatalyst, in this study, we modified WO_3 with an ionic liquid of [Bmim]I (1-butyl-3-methylimidazolium iodide) using a facile impregnation method in water at 80°C. The [Bmim]I-modified WO_3 samples were demonstrated to have much higher photocatalytic activities as compared to bare WO_3. The effects of the ionic liquid on the physicochemical properties of WO_3 and the enhanced photocatalysis were revealed in detail based on the various characterization results and analysis of the photogenerated •OH radicals in the presence and absence of soluble oxygen. To our knowledge, this is the first report on utilizing an ionic liquid modification for improving the photocatalytic activity of a narrow band gap semiconductor with a deep valence band.

2. Experimental

2.1. Regents

The chemicals that were used as received in this work included: tungsten trioxide (WO_3, 99.8%, Alfa Aesar), 1-butyl-3-methylimidazolium iodide ([Bmim]I, 99%, Lanzhou Green chem.. ILs, LICP, CAS), *tert*-butyl alcohol (TBA, AR 99%, Alfa Aesar), Rhodamine B (RhB, 99%, Acros), triethanolamine (TEOA, AR 98%, Sinopharm Chemical Reagent Beijing Co., Ltd.), terephthalic acid (AR, 98.5%, Sinopharm Chemical Reagent Beijing Co., Ltd.), and NaOH (AR, 96%, Sinopharm Chemical Reagent Beijing Co., Ltd.). Deionized water was used through the experiments. For a clear identification, the structure of the ionic liquid [Bmim]I is given in Scheme 1.

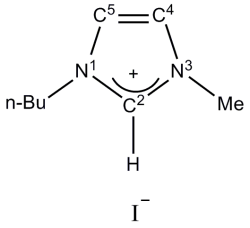

Scheme 1. Structure of 1-butyl-3-methylimidazolium iodide ([Bmim]I)

2.2. Preparation of [Bmim]I-Modified WO_3

The modification of WO_3 with [Bmim]I was carried out by using a facile impregnation method in water at 80°C. In detail, the desired amount of [Bmim]I was slowly added into 200 ml aqueous solution of NaOH (5mM). The mixture was stirred at 80°C for 0.5 hr to form an optical

transparent solution. Subsequently, 1.1593 g of WO_3 was added into the above solution. The molar ratios of [Bmim]I to WO_3 (R_{IL}) in the suspensions were set to be 0.0, 1.2, 1.5, and 1.7, respectively. The resulting suspension was then stirred at 80°C for 4 hr before naturally cooled to room temperature. The resulting precipitate was collected by centrifugation and washed with deionized water and ethanol thoroughly. Finally, the samples were dried at 80°C to form bare WO_3 (R_{IL} = 0) and [Bmim]I-modified WO_3 (denoted as IL-WO_3) with different R_{IL} values.

2.3. Characterization

X-ray diffraction (XRD) patterns of the as-prepared samples were recorded on an X-ray diffractormeter (Shimadzu, XRD-7000) using Cu Kα as X-ray radiation (λ=1.5418Å). The accelerating voltage and applied current are 40 kV and 30 mA, respectively. The morphologies were observed with a field-emission scanning electron microscope (FESEM) (JEOL, JSM-7401E). The UV-vis diffuse reflectance spectra of the samples were obtained using a spectrophotometer (Hitachi, U-3900) equipped with a diffuse reflectance accessory, and $BaSO_4$ was used as the reference. The FTIR spectra were collected with an IRPrestige-21 FTIR spectrophotometer. X-ray photoelectron spectroscopy (XPS) measurements were conducted on an ESCALAB 250Xi spectrometer with Al Kα radiation. All binding energies were referenced to the C1s peak (284.6 eV) of the surface adventitious carbon.

2.4. Photocatalytic Activity Experiments

The photocatalytic activities of the as-prepared samples were evaluated by the degradation of RhB in an aqueous solution. A total 0.01 g of the catalyst was suspended in 100 mL aqueous solution of RhB (~10^{-5} M). A 300 W Xe arc lamp (CHFXM150, Beijing Trusttech. Co. Ltd.) equipped with wavelength cutoff filter for λ > 420 nm was used as light source and positioned about 8cm above the aqueous suspension. Prior to irradiation, the suspension was magnetically stirred for an hour in the dark to ensure the establishment of the equilibrium between the catalyst surface and RhB molecules. At the given irradiation time intervals of 30 min, 5 mL of the suspension was sampled, and then the catalyst and RhB solution were separated by centrifugation. The concentration of RhB was determined by monitoring the change of the absorption spectrum in the absorbance at 554 nm with a Hitachi U-3310 spectrophotometer.

Generally, triethanolamine (TEOA) can act as an effective hole scavenger in a photocatalytic reaction, while *tert*-butyl alcohol (TBA) is •OH scavenger since it reacts with •OH radicals at a

high rate constant ($k = 6 \times 10^8$).[23] To investigate the roles of hole and •OH radical in the photocatalytic degradation of RhB over these catalysts, the degradation of RhB over these catalysts irradiated by the above light source was also evaluated in the presence of TEOA (10 mM) or TBA (10 mM) in the same manner.

2.5. Analysis of Photogenerated •OH Radicals

The photogeneration of the •OH radicals over the photo-irradiated suspensions of bare WO_3 and IL-WO_3 (R_{IL} = 1.5) in the presence or absence of soluble oxygen was measured by a fluorescence technique using terephthalic acid as a chemical trap of •OH radicals.[24] Terephthalic acid readily reacts with •OH to form 2-hydroxyterephthalic acid only (reaction 1), a significantly fluorescent product. The experimental procedure was similar to the photocatalytic activity measurements above. Briefly, the catalyst powder was suspended in the aqueous solution of terephthalic acid (0.5 mM) and NaOH (2.0 mM). Prior to irradiation, the suspension in a cuvette was magnetically stirred for an hour in the dark to ensure the establishment of the equilibrium between the catalyst surface and Terephthalic acid. At the given irradiation time intervals, 5 mL suspension was collected and filtered for fluorescence spectrum measurement. The fluorescent emission intensity of 2-hydroxyterephthalic acid was detected at 425 nm under the excitation at 315 nm using a spectrofluorometer (PerkinElmer LS55). In the case of the measurement in the absence of soluble oxygen, the suspension in a cuvette was magnetically stirred and continuously bubbled with nitrogen gas for an hour in the dark, and subsequently sealed with the cap before irradiation.

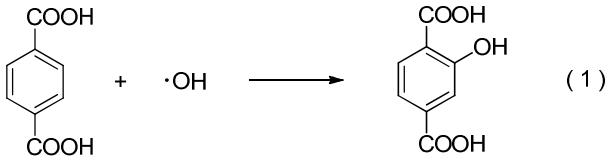

(1)

3. Results and Discussion

3.1. Physicochemical Properties

The XRD patterns of the bare WO_3 and IL-WO_3 with different R_{IL} values are displayed in Fig. 1. All samples exhibit a single monoclinic phase of well-crystallized WO_3 according to JCDS file (No. 43-1035). No other phases and changes in the full widths at half-maximum (FWHM) can be observed after the [Bmim]I modification, as is expected on the basis of the mild conditions in the

modification procedure. The results suggest that the ionic liquid modification occurs on the surface rather than the inside of WO_3 bulk, and doesn't affect the phase structure and crystallinity of WO_3. The FESEM observations (Fig. 2) show that both the bare WO_3 and IL-WO_3 (R_{IL} = 1.5) consist of dispersed large and fine particles with irregular polyhedral. The sizes of the large and fine particles are approximately 0.5~1μm and 100~300 nm, respectively. No apparent changes in the morphology and size distribution of the particles are observed after the ionic liquid modification.

Insert **Fig. 1**

Insert **Fig. 2**

The FT-IR spectra of the bare WO_3, IL-WO_3 (R_{IL} = 1.5) and [Bmim]I further evidence the presence of [Bmim]I on the surface of WO_3 (Fig. 3). In the FT-IR spectra of the bare WO_3 and IL-WO_3, the bands corresponding to the stretching vibrations of W=O and W–O bonds in WO_3 are clearly observed below 1000 cm^{-1}.[25,26] A broad band centered at 3450 cm^{-1} are associated with the stretching vibrations of hydrogen-bonded surface water molecules and hydroxyl groups.[2] It should be noted that several bands appear in the spectra of IL-WO_3 and [Bmim]I, but absent in that of the bare WO_3. Among these bands, the characteristic bands of the imidazolium ring around 3142 cm^{-1} region correspond to symmetric and asymmetric stretch of the HCCH bond in positions four and five of the imidazolium ring.[27] Other two bands at 2859 and 2926 cm^{-1} belong to alkyl chain.[28] The sharp peaks at 1580 and 1170 cm^{-1} are consistent with the in-plane deformation vibrations of the imidazolium skeleton atoms and C–H bond, respectively.[28] Furthermore, a new band at around 535 cm^{-1} was observed for IL-WO_3 only, which might be due to the formation of W–O–C bond caused by the surface modification of [Bmim]I.

Insert **Fig. 3**

The surface elemental compositions and chemical states of the bare WO_3 and IL-WO_3 (R_{IL} = 1.5) were studied by X-ray photoelectron spectroscopy (XPS). The XPS survey spectra (Fig. 4a) reveal the existence of W, O, and C elements in both samples. Fig. 4b displays the XPS spectra of W4f core levels in both samples. It can be observed that two peaks for the W4f of the bare WO_3 are located at the binding energies of 35.6 and 37.8 eV, ascribed to $W4f_{7/2}$ and $W4f_{5/2}$, respectively, which are in good agreement with those of tungsten (VI) trioxide.[29-31] Notably, the doublet is found to visibly shift toward lower binding energy after the [Bmim]I modification in the case of

IL-WO_3(R_{IL} = 1.5). This observed shift in binding energy suggests an interaction between the surface W^{6+} and $[Bmim]^+$ adsorbed on the WO_3. As shown in Fig. 4c, there are two oxygen species in both samples. The dominant peak located at around 530.3 eV is a characteristic of the lattice oxygen (O_L) in WO_3,[32,33] while the other peak at 531.3 eV could be mainly attributed to the surface oxygen (O_S) present as hydroxyl group on the surface of WO_3.[34] According to the relative XPS areas, the atomic ratio of the surface oxygen (O_S) to the total oxygen (O_L + O_S) is reduced from 29.25% to 24.81% after the modification, indicating less surface hydroxyl groups on the IL-WO_3 than on bare WO_3. Earlier investigations indicated that the surface modification of a semiconductor with ascorbic acid or ionic liquid caused a decrease in the surface hydroxyl groups.[21,22,35] The observed decrease in the surface oxygen (O_S) could be due to the replacement of some surface hydroxyl groups by the imidazolium after the modification. The peak in the C1s region of the IL-WO_3 can be deconvoluted into two contributions (Fig. 4d). They are attributed to the surface adventitious carbon (284.6 eV) and the carbon (286.2 eV) in the C-N groups of imidazolium, respectively.[36,37] FT-IR and XPS studies therefore allow us to conclude that the ionic liquid is bound to the surface of WO_3 substrate.

Insert **Fig. 4**

The optical properties of these samples were investigated by UV-vis diffuse reflectance spectroscopy, as shown in Fig. 5. All samples exhibit an intense absorption starting at around 475 nm, which corresponds to the band gap absorption of WO_3. Differently, UV-vis absorbance in the range of the wavelengths shorter than 475 nm is gradually enhanced with the increase in R_{IL} value. A similar phenomenon was also reported for [Bmim]I-modified BiOI.[22]

Insert **Fig. 5**

3.2. Photocatalytic Behaviors

RhB is one of the representative organic dyes and has been widely chosen as a degraded target in the evaluation of photocatalytic activity.[38] To investigate the effects of the modification of [Bmim]I on the photocatalytic performance of WO_3, thus, the photocatalytic activities of bare WO_3 and IL-WO_3 with different R_{IL} values were evaluated by the degradation of RhB under the visible light irradiation ($\lambda > 420$), as shown in Fig. 6. It can be clearly observed that the self-degradation of RhB is negligible under the visible light irradiation in the presence of no catalyst. All IL-WO_3 samples exhibit much higher photocatalytic activities than bare WO_3,

demonstrating that the [Bmim]I modification is an effective way to enhance the photocatalysis of WO_3. The poor photocatalytic activity of bare WO_3 could be attributed to a fast recombination of photogenerated electron-hole pairs since the multi-electron reduction of dioxygen is much less efficient than one-electron reduction of dioxygen, as mentioned above. The highest RhB degradation yield occurs over the IL-WO_3 (R_{IL} = 1.5). Approximately 83% RhB degradation is achieved over this sample after the visible light irradiation for 3 h, as compared to less than 30% RhB degradation over bare WO_3 within the same irradiation time. Moreover, the degradation yield of RhB over the IL-WO_3 (R_{IL} = 1.7) starts to drop although it is still higher than that over bare WO_3. This might be due to the coverage of the WO_3 surface by excess [Bmim]I, leading to a decrease in the surface active sites for RhB absorption.

Insert **Fig. 6**

Insert **Fig. 7**

We then investigated the effects of different scavenges on the degradation of RhB over bare WO_3 and IL-WO_3 (R_{IL} = 1.5) under the visible light irradiation ($\lambda > 420$). As shown in Fig. 7, over both samples, the degradation efficiency of RhB almost falls to half of the original with the addition of •OH scavenger TBA, and almost no degradation of RhB are observed when TEOA, an effective hole scavenger, is added into the photocatalytic reaction solution. These results reveal that both the photogenerated hole and •OH radical as oxidation species play equivalent roles in the degradation of RhB in both systems. From the viewpoint of thermodynamics, the electron photoexcited on the conduction band of WO_3 (+0.3~0.5 V vs NHE) is energetically capable of reducing oxygen molecules to form H_2O_2 through two-electron reduction process [reaction 2, $E^o(O_2/H_2O_2)$ = + 0.695 V vs NHE]. Thus, over both bare WO_3 and IL-WO_3, the •OH radicals could be also produced through the reductive path of the conduction band electron (reaction 3) in addition to the direct reaction of the valence band hole with surface water or hydroxyl group (reaction 4).

$$2e_{CB}^- + O_2 + 2H^+ \rightarrow H_2O_2 \qquad (2)$$

$$H_2O_2 + e_{CB}^- \rightarrow OH^- + \bullet OH \qquad (3)$$

$$h_{VB}^+ + H_2O \text{ (or } -OH) \rightarrow \bullet OH \qquad (4)$$

Both •OH radical and hole photogenerated over WO_3 can degrade almost all organic compounds due to their high redox potentials (+2.7 V and +3.1 V vs NHE, respectively). Thus, no degradation of RhB occurring over both samples in the presence of TEOA rules out the possibility of the •OH

radical production through reaction 3. This means that the photogenerated holes in both samples are totally responsible for both the direct degradation of RhB and production of •OH radical (reaction 4), as a result, influence the final photocatalytic properties. Based on the photocatalytic performances of bare WO_3 and IL-WO_3 in Fig. 6, therefore, it could be concluded that the production yield of photogenerated holes should be much higher over bare WO_3 than over IL-WO_3.

Insert **Fig. 8**

Furthermore, the photocatalytic stability and reusability of the IL-WO_3 catalyst was checked by performing the cyclic degradation process of fresh RhB solution with the used catalyst from the previous runs under the same conditions. As shown in Fig. 8, the IL-WO_3 (R_{IL} = 1.5) catalyst can be effectively recycled at least four times without an obvious decrease in its photocatalytic activity. This result supports that the catalyst is sufficiently stable. In other words, the [Bmim]I is strongly bound to the surface of the WO_3 substrate and not degraded during the photocatalytic degradation of pollutants, which is critical for a practical application.

3.3. Photogeneration of •OH Radicals

The hydroxyl radicals (•OH) formed in the visible light irradiated suspensions of bare WO_3 and IL-WO_3 (R_{IL} = 1.5) were detected by a fluorescence technique using terephthalic acid as a chemical trap of •OH radical, as shown in Fig. 9a and 9b. It can be observed that the fluorescence emission signals of 2-hydroxyterephthalic acid at about 425 nm are produced for both samples, suggesting the production of •OH radicals. The production of •OH radicals is much more over IL-WO_3 (R_{IL} = 1.5) than over bare WO_3 within the same irradiation time. This result parallels the photocatalytic performances of two samples shown in Fig. 6 and 7. It was revealed in Fig. 7 that the production of the •OH radicals over two samples are originated from the direct reaction of the valence band hole with surface water or hydroxyl group (reaction 4) only. According to the characterization results above, the ionic liquid [Bmim]I is tightly bound to the surface of the WO_3, and no changes in the properties of the WO_3 bulk occur after the [Bmim]I modification. Moreover, the modification also causes an obvious decrease in the surface hydroxyl groups, as confirmed by the XPS analysis above. As a result, it can be concluded that an efficient separation of the electron-hole pairs photoexcited over the WO_3 has been successfully achieved after the surface modification with [Bmim]I.

It was well known that the unique properties of [Bmim]I are largely related to its electronic structure of the aromatic cations (Scheme 1).[39] This electronic structure comprises a delocalized 3-center-4-electron configuration across the N1-C2-N3 moiety, a double bond between C4 and C5 at the opposite side of the ring, and a weak delocalization in the central region.[40] With such an electronic structure, the surface-bound imidazolium ring could act as an electron-trapping group to stabilize an external electron through a conjugation effect.[41] In other words, due to the conjugation effect in the imidazolium ring, the [Bmim]I modification endows the surface of WO_3 with a stronger capability to stabilize the electron photoexcited at the conduction band. The electron stabilization on the surface-bound $[Bmim]^+$ retards the photoexcited electron transfer to surface, probably forming H_2O_2 or H_2O through multi-electron reduction process, but the recombination of the photoexcited electron-hole pair is effectively suppressed to a great extent. Consequently, more holes photoexcited over IL-WO_3 are allowed to react with surface water or hydroxyl groups to form hydroxyl radicals, or directly degrade the organic compound, which greatly enhances the photocatalytic efficiencies.

Insert **Fig. 9**

To provide a more convincing evidence for the capability of the surface-bound $[Bmim]^+$ as an electron-trapping group to inhibit the recombination of the electron-hole pairs photoexcited over IL-WO_3, we also detected the •OH radicals formed in the visible light irradiated suspensions of bare WO_3 and IL-WO_3 (R_{IL} = 1.5) in the absence of soluble oxygen using the same manner. According to the fluorescent emission spectra shown in Fig. 9c and 9d, the production of •OH radicals is negligible over bare WO_3 under the visible light irradiation. This is due to a fast charge recombination in the absence of soluble oxygen as an electron scavenger. In the case of the IL-WO_3 (R_{IL} = 1.5), amazingly, the •OH radicals apparently increases with the irradiation time. This indicates that the separation of the photoexcited electron-hole pairs can be still achieved over the IL-WO_3 in the absence of soluble oxygen as an electron scavenger, allowing the holes to react with water or surface hydroxyl groups to form hydroxyl radicals. The charge separation occurring over IL-WO_3 in the absence of soluble oxygen is only attributed to the electron-trapping effect of the surface-bound $[Bmim]^+$. The •OH radical measurements well clarify the electron-trapping capability of the imidazolium ring bound to the surface of WO_3, and well support the above understanding of the enhanced photocatalysis over IL-WO_3.

In summary, we demonstrated that the photocatalytic activity of WO_3 can be significantly enhanced after the surface modification of an ionic liquid [Bmim]I through a facile impregnation method. Various characterization results showed that the [Bmim]I is tightly bound to the surface of WO_3. It was revealed that the presence of the surface-bound $[Bmim]^+$ could effectively inhibit the recombination of photogenerated electron-hole pairs by trapping the electrons photoexcited on the conduction band, which is responsible for the observed enhancement of the photocatalysis. In addition, the [Bmim]I-modified WO_3 exhibits sufficient stability and long-lasting photocatalytic activity, which allows it for a practical application. This work, we believe, would pave a way for the development of the narrow band gap semiconductors with a deep valence band as efficient visible light photocatalytic materials.

Acknowledgements

This work was supported by National Natural Science Foundation of China (No.21273281) and National Basic Research Program of China (973 Program, No.2013CB632405).

References

1 X. C. Wang, K. Maeda, A. Thomas, K. Takanabe, G. Xin, J. M. Carlsson, K. Domen and M. Antonietti, *Nat. Mater.*, 2009, **8**, 76-80.

2 H.-Y. Jiang, J. Liu, K. Cheng, W. Sun and J. Lin, *J. Phys. Chem. C*, 2013, **117**, 20029-20036.

3 J. Low, J. Yu, Q. Li and B. Cheng, *Phys. Chem. Chem. Phys.*, 2014, **16**, 1111-1120.

4 C. Santato, M. Ulmann and J. Augustynski, *Adv. Mater.*, 2001, **13**, 511-514.

5 M. Sadakane, K. Sakaki, H. Kunioku, B. Ohtani, W. Ueda and R. Abe, *Chem. Commun.*, 2008, 6552-6554.

6 G. R. Bamwenda, T. Uesigi, Y. Abe, K. Sayama and H. Arakawa, *Appl. Catal. A*, 2001, **205**, 117-128.

7 W. Morales, M. Cason, O. Aina, N. R. de. Tacconi and K. Rajeshwar, *J. Am. Chem. Soc.*, 2008, **130**, 6318-6319.

8 J. Yu, L. Qi, B. Cheng and X. Zhao, *J. Hazard. Mater.*, 2008, **160**, 621-628.

9 R. Abe, H. Takami, N. Murakami and B. Ohtani, *J. Am. Chem. Soc.*, 2008, **130**, 7780-7781.

10 J. Kim, C. W. Lee and W. Choi, *Environ. Sci. Technol.*, 2010, **44**, 6849-6854.

11 Z.-G. Zhao and M. Miyauchi, *Angew. Chem., Int. Ed.*, 2008, **47**, 7051-7055.

12 T. Arai, M. Horiguchi, M. Yanagida, T. Gunji, H. Sugihara and K. Sayama, *Chem. Commun.*,

2008, 5565-5567.

13 A. Tanaka, K. Hashimoto and H. Kominami, *J. Am. Chem. Soc.*, 2014, **136**, 586-589.

14 T. Arai, M. Horiguchi, M. Yanagida, T. Gunji, H. Sugihara and K. Sayama. *J. Phys. Chem. C*, 2009, **113**, 6602-6609.

15 Y. Nosaka, S. Takashi, H. Sakamoto and A. Y. Nosaka, *J. Phys. Chem. C*, 2011, **115**, 21283-21290.

16 X. An, J. C. Yu, Y. Wang, Y. Hu, X. Yu and G. Zhang, *J. Mater. Chem.*, 2012, **22**, 8525-8531.

17 Z.-G. Zhao and M. Miyauchi, *J. Phys. Chem. C*, 2009, **113**, 6539-6546.

18 T. Welton, *Chem. Rev.*, 1999, **99**, 2071-2083.

19 R. Katoh, M. Hara and S. Tsuzuki, *J. Phys. Chem. B*, 2008, **112**, 15426.

20 X. Meng and F.-S. Xiao, *Chem. Rev.*, 2014, **114**, 1521-1543.

21 S. Hu, A. Wang, X. Li, Y. Wang and H. Löwe, *Chem. Asian J.*, 2010, **5**, 1171-1177.

22 Y. Wang, K. Deng and L. Zhang, *J. Phys. Chem. C* 2011, **115**, 14300-14308.

23 G. V. Buxton, C. L. Greenstock, W. P. Helman and A. B. Ross, *J. Phys. Chem. Ref. Data*, 1988, **17**, 513-886.

24 K. Ishibashi, A. Fujishima, T. Watanabe and K. Hashimoto, *Electrochem. Commun.* 2000, **2**, 207-210.

25 M. Breedon, P. Spizzirri, M. Taylor, J. du Plessis, D. McCulloch, J. Zhu, L. Yu, Z. Hu, C. Rix, W. Wlodariski and K. Kalantarzadeh, *Cryst. Growth Des.*, 2010, **10**, 430-439.

26 A. Baserga, V. Russo, F. Difonzo, A. Bailini, D. Cattaneo, C. Casari, A. Libassi and C. Bottani, *Thin Solid Films*, 2007, **515**, 6465-6469.

27 B. Fitchett and J. C. Conboy, *J. Phys. Chem. B*, 2004, **108**, 20225-20262.

28 T. Wang, H. Kaper, M. Antonietti and B. Smarsly, *Langmuir*, 2007, **23**, 1489-1495.

29 R. J. Colton and J. W. Rabalais, *Inorg. Chem.*, 1976, **15**, 236-238.

30 Y. Baek and K. Yong, *J. Phys. Chem. C*, 2007, **111**, 1213-1218.

31 J. N. Yao, P. Chen and A. Fujishima, *Electroanal. Chem.*, 1996, **406**, 223-226.

32 S. B. Bon, L. Valentini, R. Verdejo, J. L. G. Fierro, L. Peponi, M. A. Lopez-Manchada and J. M. Kenny, *Chem. Mater.*, 2009, **21**, 3433-3438.

33 J. Qin, M. Cao, N. Li and C. Hu, *J. Mater. Chem.*, 2011, **21**, 17167-17174.

34 Y. W. Wang, Y. Huang, W. K. Ho, L. Z. Zhang, Z. G. Zou and S. C. Lee, *J. Hazard. Mater.*,

2009, **169**, 77-87.

35 Y. Ou, J. D. Lin, H. M. Zou and D. W. Liao, *J. Mol. Catal. A Chem.*, 2005, **241**, 59-64.

36 S. Biniak, G. Szymanski, J. Siedlewski and A. Swiatkowski, *Carbon*, 1997, **35**, 1799-1810.

37 X. Tang, Y. Li, X. Huang, Y. Xu, H. Zhu, J. Wang and W. Shen, *Appl. Catal. B: Environ.*, 2006, **62**, 265-273.

38 J. S. Chen, J. Liu, S. Z. Qiao, R. Xu and X. W. Lou. *Chem. Commun*., **47**, 10443-10445.

39 H. Weingartner, *Angew. Chem. Int. Ed.*, 2008, **47**, 654-670.

40 P. A. Hunt, B. Kirchmer and T. Welton. *Chem. Eur. J.*, 2006, **12**, 6762-6775.

41 R. T. Morrison and R. N. Boyd, *Organic Chemistry*, Allyn and Bacon, London, 4th edn., 1983.

Figures and Captions

Captions of Figures

Fig. 1 X-ray diffraction patterns of bare WO_3 and IL-WO_3 with different R_{IL} values.

Fig. 2 FESEM images of bare WO_3 (a) and IL-WO_3 (R_{IL} = 1.5) (b).

Fig. 3 FT-IR spectra of bare WO_3, IL-WO_3 (R_{IL} = 1.5) and [Bmim]I.

Fig. 4 XPS survey spectra of bare WO_3 and IL-WO_3 (R_{IL} = 1.5) (a). High-resolution XPS spectra of bare WO_3 and IL-WO_3 (R_{IL} = 1.5) in the regions of W4f (b), O1s (c) and C1s (d).

Fig. 5 UV-vis diffuse reflectance spectra of bare WO_3 and IL-WO_3 with different R_{IL} values.

Fig. 6 Photocatalytic degradation yields of RhB over bare WO_3 and IL-WO_3 with different R_{IL} values under visible light irradiation ($\lambda > 420$) for 3 h.

Fig. 7 Photocatalytic degradation of RhB over bare WO_3 and IL-WO_3 (R_{IL} = 1.5) in the presence and absence of different scavenges under visible light irradiation.

Fig. 8 Cyclic use of IL-WO_3 (R_{IL} = 1.5) for the photocatalytic degradation of RhB.

Fig. 9 Fluorescent emission intensities of the 2-hydroxyterephthalic acid produced in the visible light irradiated suspensions of bare WO_3 and IL-WO_3 (R_{IL} = 1.5) in the presence (a and b) absence (b and d) of soluble oxygen.

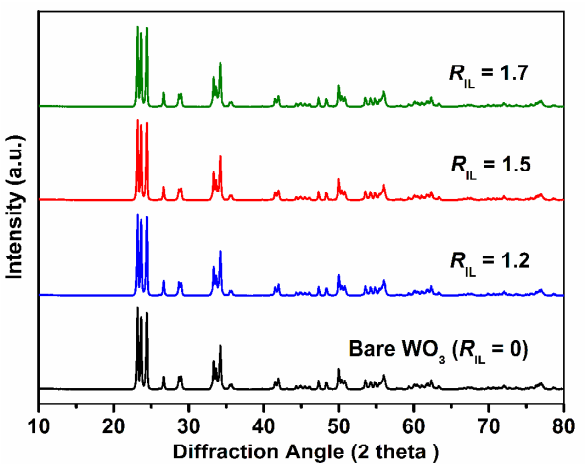

Fig. 1

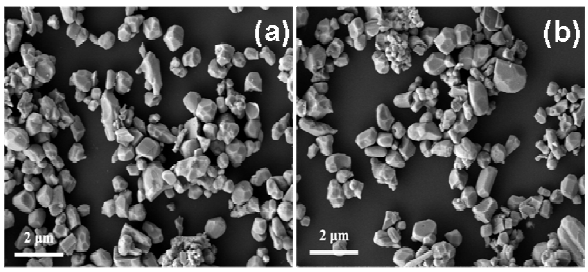

Fig. 2

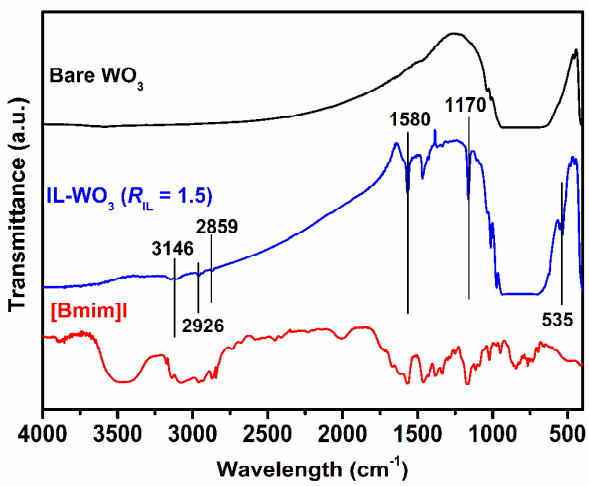

Fig. 3

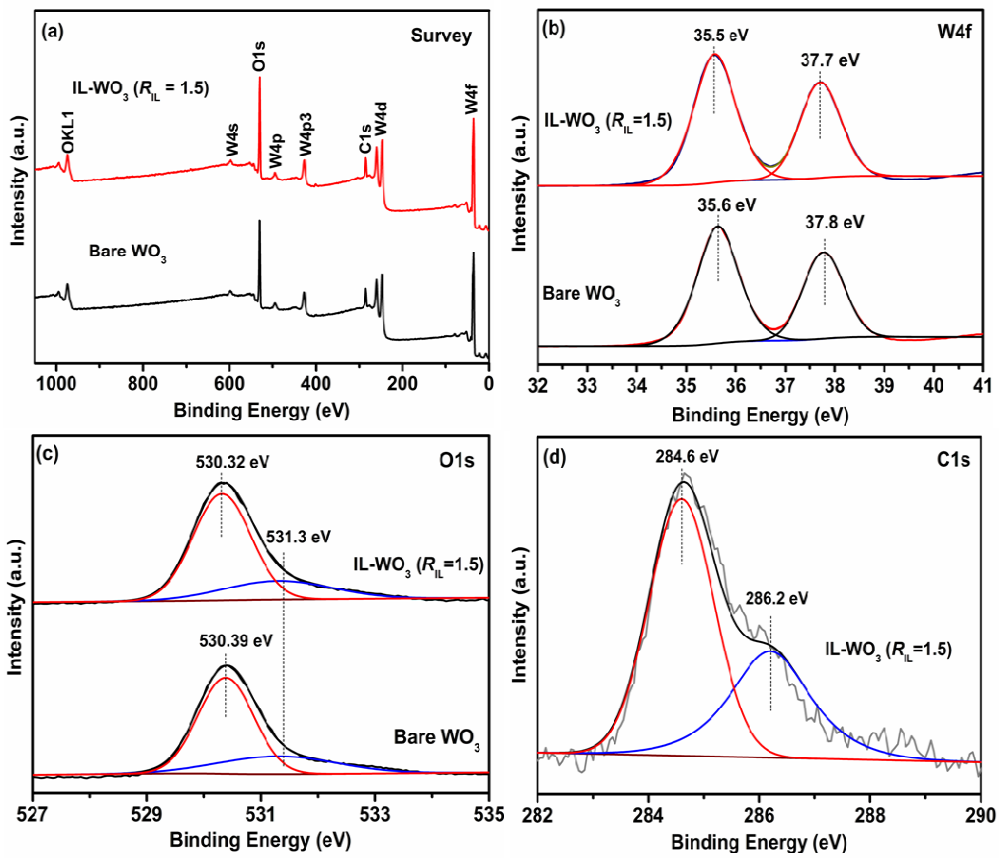

Fig. 4

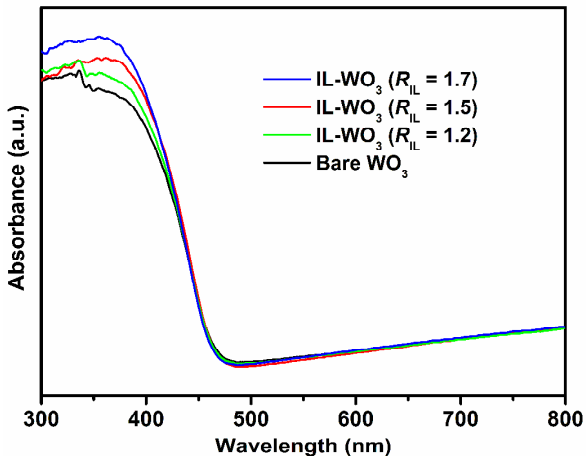

Fig. 5

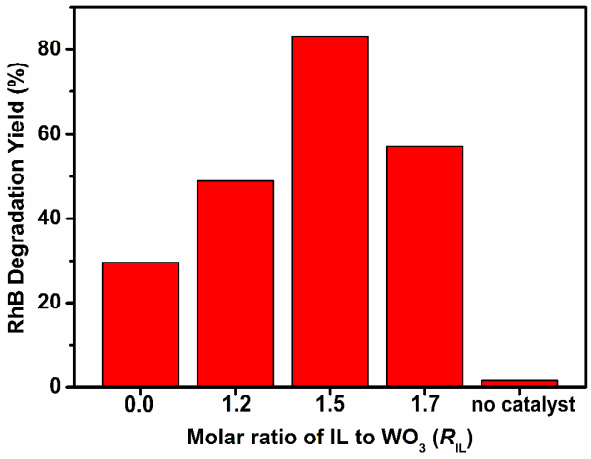

Fig. 6

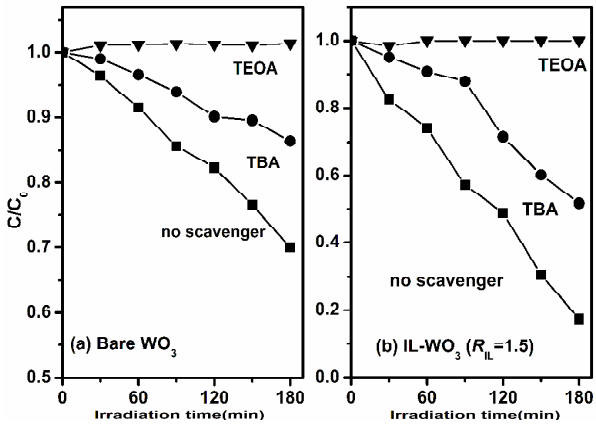

Fig. 7

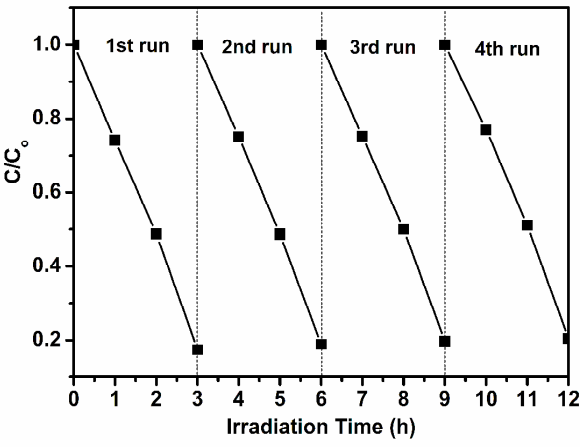

Fig. 8

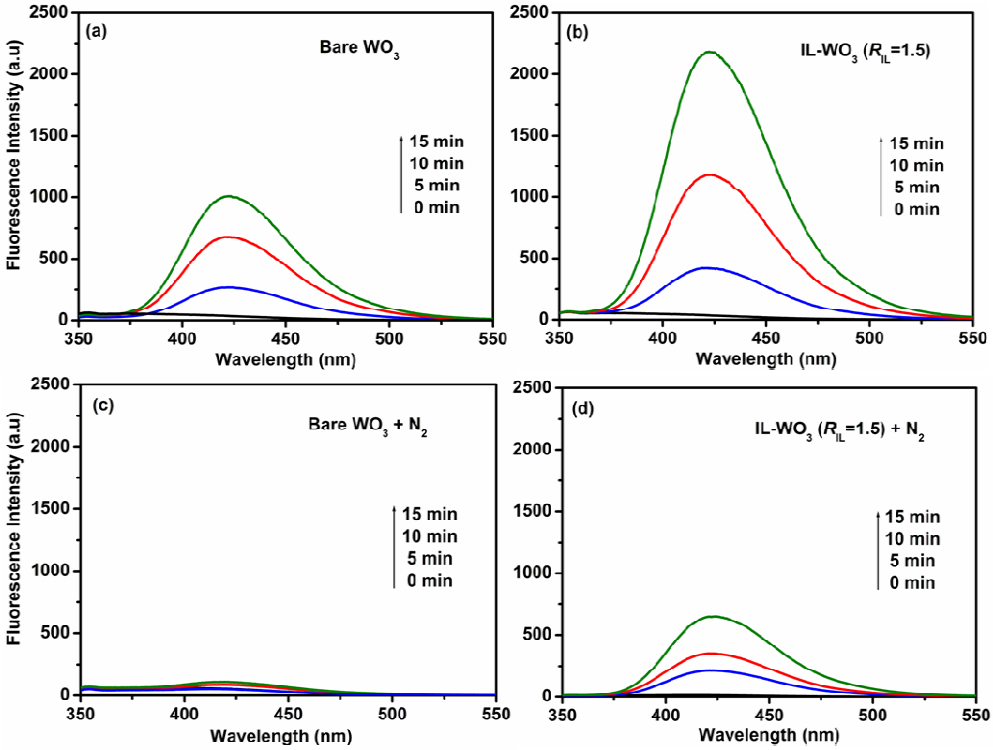

Fig. 9